bioRxiv preprint doi: https://doi.org/10.1101/703421; this version posted July 16, 2019. The copyright holder for this preprint (which was not certified by peer review) is the author/funder, who has granted bioRxiv a license to display the preprint in perpetuity. It is made available under aCC-BY 4.0 International license.

Whole-chromosome hitchhiking driven by a male-killing endosymbiont

Simon H. Martin*[1,2], Kumar Saurabh Singh[3], Ian J. Gordon[4], Kennedy Saitoti Omufwoko[5,6], Steve Collins[7], Ian A Warren[1], Hannah Munby[1], Oskar Brattström[1], Walther Traut[8], Dino J. Martins[5,6], David A. S. Smith[9], Chris D. Jiggins[1], Chris Bass[3], Richard H. ffrench-Constant[3]

[1]Department of Zoology, University of Cambridge, Cambridge, CB2 3EJ, United Kingdom

[2]Institute of Evolutionary Biology, University of Edinburgh, Edinburgh EH9 3FL, United Kingdom

[3]Centre for Ecology and Conservation, University of Exeter, Penryn Campus, Penryn, TR10 9EZ, United Kingdom

[4]BirdLife International Kigali Office, Box 2527, Kigali Post Office, Kigali, Rwanda

[5]Mpala Research Centre, P O Box 555, Nanyuki, 10400 Kenya.

[6]Department of Ecology and Evolutionary Biology, Princeton University, Princeton, NJ 08544, USA

[7]African Butterfly Research Institute, Box 14308-0800, Nairobi, Kenya

[8]Institut für Biologie, Zentrum für medizinische Struktur- und Zellbiologie, Universität Lübeck, Ratzeburger Allee 160, 23538 Lübeck, Germany

[9]Natural History Museum, Eton College, Windsor SL4 6DW, UK

*Correspondence to: simon.martin@ed.ac.uk

bioRxiv preprint doi: https://doi.org/10.1101/703421; this version posted July 16, 2019. The copyright holder for this preprint (which was not certified by peer review) is the author/funder, who has granted bioRxiv a license to display the preprint in perpetuity. It is made available under aCC-BY 4.0 International license.

Abstract

Neo-sex chromosomes are found in many taxa, but the forces driving their emergence and spread are poorly understood. The female-specific neo-W chromosome of the African monarch (or queen) butterfly *Danaus chrysippus* presents an intriguing case study because it is restricted to a single 'contact zone' population, involves a putative colour patterning supergene, and co-occurs with infection by the the male-killing endosymbiont *Sprioplasma*. We investigated the origin and evolution of this system using whole genome sequencing. We first identify the 'BC supergene', a large region of suppressed recombination that links two colour patterning loci. Association analysis suggests that the genes *yellow* and *arrow* control the forewing colour pattern differences between *D. chrysippus* subspecies. We then show that the same chromosome has recently formed a neo-W that has spread through the contact zone within ~2200 years. We also assembled the genome of the male-killing *Spiroplasma*, and find that it shows perfect genealogical congruence with the neo-W, suggesting that the neo-W has hitchhiked to high frequency as the male killer has spread through the population. The complete absence of female crossing-over in the Lepidoptera causes whole-chromosome hitchhiking of a single neo-W haplotype, carrying a single allele of the BC supergene, and dragging multiple non-synonymous mutations to high frequency. This has created a population of infected females that all carry the same recessive colour patterning allele, making the phenotypes of each successive generation highly dependent on uninfected male immigrants. Our findings show how hitchhiking can occur between the unlinked genomes of host and endosymbiont, with dramatic consequences.

bioRxiv preprint doi: https://doi.org/10.1101/703421; this version posted July 16, 2019. The copyright holder for this preprint (which was not certified by peer review) is the author/funder, who has granted bioRxiv a license to display the preprint in perpetuity. It is made available under aCC-BY 4.0 International license.

Introduction

Structural changes to the genome play an important role in evolution by altering the extent of recombination among loci. This is best studied in the context of chromosomal inversions that cause localised recombination suppression, and can be favoured by selection if they help to maintain clusters of co-adapted alleles (or 'supergenes') in the face of genetic mixing [1–4]. A greater extent of recombination suppression occurs in the formation of heteromorphic sex chromosomes, which can link sex-specific alleles in a similarly to supergenes [5]. However, suppressed recombination can also have costs. In particular, male-specific Y and female-specific W chromosomes can be entirely devoid of recombination, making them vulnerable to genetic hitchhiking and the accumulation of deleterious mutations through 'Muller's ratchet', which may explain their deterioration over time [6–8]. These contrasting benefits and costs of recombination suppression are of particular interest in the evolution of neo-sex chromosomes, which can form through fusion of autosomes to existing sex chromosomes. There is accumulating evidence that neo-sex chromosomes are common in animals [9–15], but the processes underlying their emergence, spread and subsequent evolution have not been widely studied. In particular, there are few studied examples of recently-formed neo-sex chromosomes that are not yet fixed in a species.

The African monarch (or queen) butterfly *Danaus chrysippus*, provides a unique test case for the causes and consequences of changes in genome architecture. Like its American cousin (*D. plexippus*), it feeds on milkweeds and has bright colour patterns that warn predators of its distastefulness. However, within Africa *D. chrysippus* is divided into four subspecies with distinct colour patterns and largely distinct ranges (Fig. 1A). Predator learning should favour the maintenance of a single monomorphic warning in any single area. For this reason, researchers have long been puzzled by the large polymorphic contact zone in East and Central Africa, where all four *D. chrysippus* subspecies meet and interbreed [16–18] (Fig. 1A). Crosses have shown that colour pattern differences between the subspecies are controlled by Mendelian autosomal loci, including the tightly linked 'B' and 'C' loci (putatively a 'BC supergene' [19]) that define three common forewing patterns [20,21] (Fig. 1B). However, crosses with females from the contact zone revealed that the BC chromosome has become sex linked, forming a neo-W that is unique to this population [19,22]. Since female meiosis is achiasmatic (it lacks crossing-over) in the Lepidoptera, the formation of a neo-W would instantaneously cause perfect linkage, not just

bioRxiv preprint doi: https://doi.org/10.1101/703421; this version posted July 16, 2019. The copyright holder for this preprint (which was not certified by peer review) is the author/funder, who has granted bioRxiv a license to display the preprint in perpetuity. It is made available under aCC-BY 4.0 International license.

of the B and C loci, but of an entire non-recombining chromosome, along with other maternally-inherited DNA.

What is particularly striking is that the presence of the neo-W coincides with infection by a maternally-inherited 'male killer' endosymbiont related to *Spiroplasma ixodetis,* which kills male offspring and leads to highly female-biased populations in the contact zone [22–24]. The combination of neo-W and male killing is expected to dramatically alter the inheritance and evolution of the BC chromosome [22,25]: Infected females typically give rise to all-female broods who should always inherit the same colour patterning allele on their neo-W, along with the male-killer, while the other maternal allele is systematically eliminated in the dead sons (Fig. 1C), forming a genetic sink for all colour pattern alleles not on the neo-W. It has been suggested that the restriction of male killing to females with the neo-W, and only in the region in which hybridisation occurs between subspecies, may not be a coincidence [19,22,25–27]. However, the genomic underpinnings of this system, including the genetic controllers of colour pattern, the source and spread of the neo-W, and its relationship with the male killer, have until now remained a mystery. We generated a reference genome for *D. chrysippus* and used whole genome sequencing of population samples to uncover the interconnected evolution of the BC supergene, neo-W and *Spiroplasma.* Our findings reveal a recent whole-chromosome selective sweep caused by hitchhiking between the host and endosymbiont genomes.

bioRxiv preprint doi: https://doi.org/10.1101/703421; this version posted July 16, 2019. The copyright holder for this preprint (which was not certified by peer review) is the author/funder, who has granted bioRxiv a license to display the preprint in perpetuity. It is made available under aCC-BY 4.0 International license.

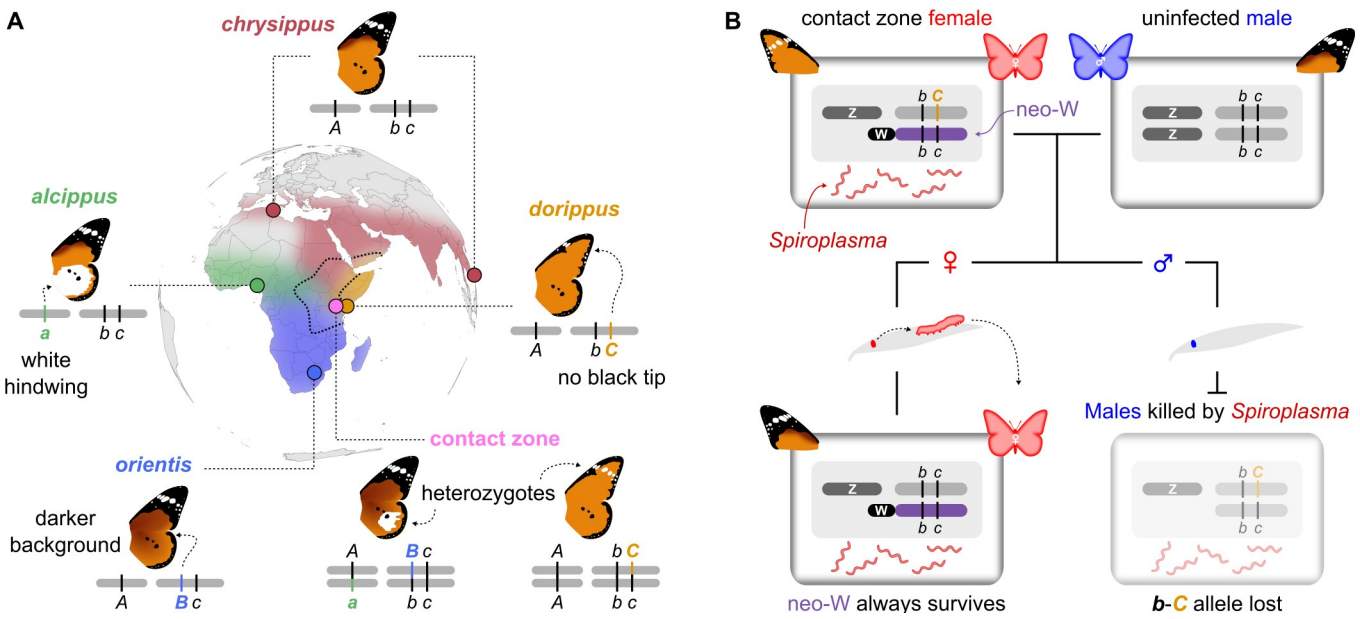

Fig. 1. Geography and genetics of colour pattern. (**A**) Approximate ranges of the four subspecies of *D. chrysippus*, with the contact zone outlined. Sampling locations for each of the subspecies and the contact zone are indicated. Cartoon chromosomes show the genotypes of each subspecies at the A (white hindwing patch), B (brown background colour) and C (forewing tip) colour patterning loci, based on previous crosses [20]. Note the linkage of B and C, putatively forming a 'BC supergene' [19]. Two examples of heterozygotes that can be found in the contact zone are shown. Note that *Cc* heterozygotes can exhibit the *transiens* phenotype with white markings on the forewing with ~50% penetrance. (**B**) Model showing how fusion of the BC autosome to the W chromosome has produced a neo-W (purple) in contact zone females (top left), while males have two autosomal copies of the BC chromosome (top right). Daughters inherit the neo-W, while sons inherit the other BC chromosome haplotype from their mother. The latter allele is then lost due to male killing by *Spiroplasma*.

Results and Discussion

Identification of the BC supergene

We assembled a high quality draft genome for *D. chrysippus,* with a total length of 322 Megabases (Mb), a scaffold N50 length of 0.63 Mb, and a BUSCO [28] completeness score of 94% (Table S1-S8). We then further scaffolded the genome into a pseudo-chromosomal assembly based on homology with the *Heliconius melpomene* genome [29–31] accounting for known fusions that differentiate these species [9,30,32] (Fig. S1). We also re-sequenced 42 individuals representing monomorphic populations of each of the four subspecies and a polymorphic population from a known male-killing hotspot near Nairobi, in the contact zone (Fig 1A, Table S9).

bioRxiv preprint doi: https://doi.org/10.1101/703421; this version posted July 16, 2019. The copyright holder for this preprint (which was not certified by peer review) is the author/funder, who has granted bioRxiv a license to display the preprint in perpetuity. It is made available under aCC-BY 4.0 International license.

To identify the putative BC supergene, we scanned for genomic regions showing high differentiation between the subspecies and an association with colour pattern. Genetic differentiation (F_{ST}) is largely restricted to a handful of broad peaks, with a background level of approximately zero (Fig. 2, S2). This low background level implies a large and nearly panmictic population. Indeed, average genome-wide diversity at putatively neutral 4-fold degenerate 3rd codon positions is 0.042, which is the highest value reported for any arthropod to our knowledge [33], indicating an extremely large effective population size. The islands of differentiation that stand out from this background imply selection for local adaptation maintaining particular differences between the subspecies, similar to patterns seen between geographic races of *Heliconius* butterflies [34]. However, here the peaks of differentiation are broad, covering several Mb, implying some mechanism of recombination suppression such as inversions that differentiate the subspecies.

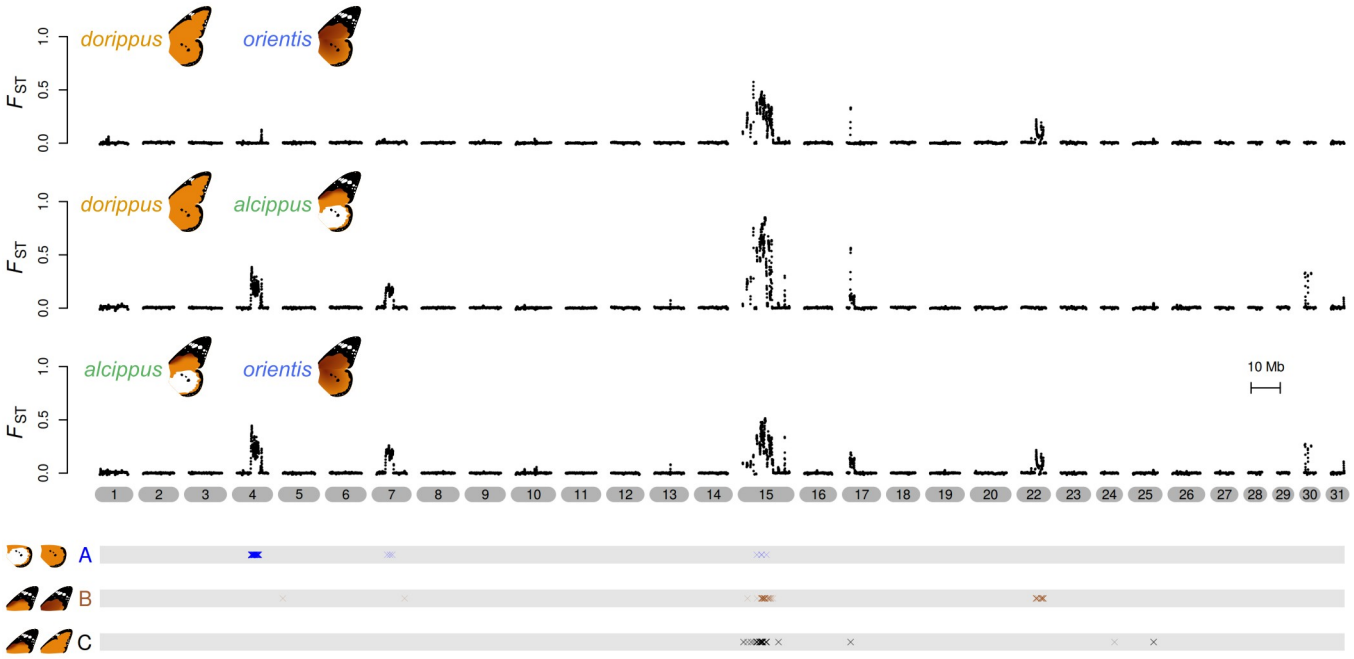

Fig. 2. Genetic differentiation and associations with colour pattern. Pairwise genetic differentiation (F_{ST}), plotted in 100 kb sliding windows with a step size of 20 kb across all chromosomes. Three different pairs of subspecies for which sample sizes were ≥ 6 are shown. F_{ST} of ~0 indicates a lack of genetic differentiation between populations, and peaks indicate strong differentiation. Below, locations of SNPs most strongly associated with the A, B and C loci are shown (Wald test, 99.99% quantile). See Fig. S2 for a more detailed plot.

bioRxiv preprint doi: https://doi.org/10.1101/703421; this version posted July 16, 2019. The copyright holder for this preprint (which was not certified by peer review) is the author/funder, who has granted bioRxiv a license to display the preprint in perpetuity. It is made available under aCC-BY 4.0 International license.

The inclusion of the polymorphic contact-zone samples, and the fact that three of the subspecies each carry a unique colour pattern allele (Fig. 1A), allowed us to identify particular differentiated regions associated with the three major colour pattern traits. A ~3 Mb region on chromosome 4 is associated with the white hindwing patch (A locus) and a ~5 Mb region on chromosome 15 (hereafter chr15) is associated with both background colour (B locus) and the forewing black tip (C locus) (Fig. 2, S2). Below, we refer to this region on chr15, which spans over 200 protein-coding genes, as the BC supergene [19], although we note that additional associated SNPs on chromosome 22 suggest that background wing melanism may also be influenced by other loci.

Clustering analysis based on genetic distances reveals three clearly distinct alleles at the BC supergene (Fig 3A). This further supports the hypothesis of recombination suppression, although a number of individuals show mosaic patterns consistent with rare recombination (Fig S3). The three main alleles correspond to the three common forewing phenotypes, so we term these $BC^{chrysippus}$ (orange background with black forewing tip, formerly *bbcc*), $BC^{dorippus}$ (orange without black tip, formerly *bbCC*), and $BC^{orientis}$ (brown background with black forewing tip, formerly *BBcc*) (Fig 3A). Fifteen of the twenty contact zone individuals are heterozygous, carrying two distinct BC alleles, and a few show evidence for recombination, as is also seen in some of the southern African *orientis* individuals (Fig. S3). As shown previously, $BC^{dorippus}$ (which includes the dominant *C* allele) and $BC^{orientis}$ (which includes the dominant *B* allele) are both dominant over the recessive $BC^{chrysippus}$ (Fig. 3A, S3).

bioRxiv preprint doi: https://doi.org/10.1101/703421; this version posted July 16, 2019. The copyright holder for this preprint (which was not certified by peer review) is the author/funder, who has granted bioRxiv a license to display the preprint in perpetuity. It is made available under aCC-BY 4.0 International license.

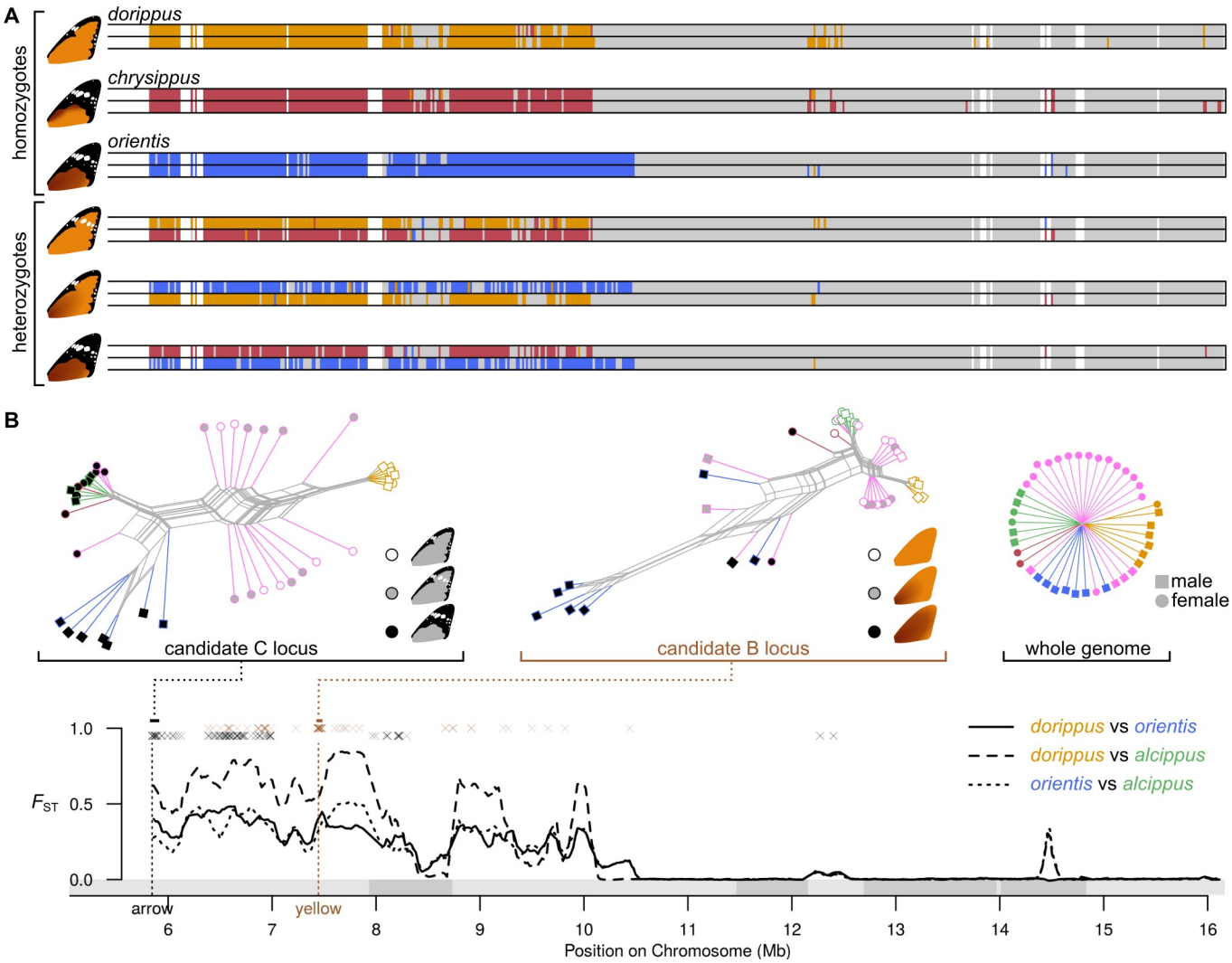

148 **Fig. 3. Identification of the BC supergene on chromosome 15.** (**A**) Allelic clustering on
149 chromosome 15 (chr15) in six representative individuals (see Fig. S3 for all individuals, and see
150 panel B for chromosome positions). Coloured blocks indicate 20 kb windows in which sequence
151 haplotypes could be assigned to one of three clusters based on pairwise genetic distances (see
152 Methods for details). Windows in grey show insufficient relative divergence to be assigned to a
153 cluster and white indicates missing data. (**B**) Genetic differentiation (F_{ST}; bottom) among three
154 subspecies pairs across chr15. Note that the first ~6 Mb of the chromosome is not shown due to
155 complex structural variation (see main text). Scaffolds are indicated below the plot in alternating
156 shades of grey. Above the plot, locations of SNPs most strongly associated with the B and C loci
157 (Wald test, 99.99% quantile) are shown in brown and black, respectively. Distance-based
158 phylogenetic networks constructed for candidate regions for the B and C loci are also shown,
159 along with a corresponding network for the whole genome for contrast. Colours indicate
160 subspecies as in Fig. 1A, and shapes indicate sex. Phenotypes for B and C are coded black and
161 white for putative homozygotes and gray for putative heterozygotes. The locations of our most
162 likely candidate genes for B (*yellow*) and C (*arrow*) are indicated.

bioRxiv preprint doi: https://doi.org/10.1101/703421; this version posted July 16, 2019. The copyright holder for this preprint (which was not certified by peer review) is the author/funder, who has granted bioRxiv a license to display the preprint in perpetuity. It is made available under aCC-BY 4.0 International license.

Although it can be challenging to identify particular functional mutations in regions of suppressed recombination, the presence of some recombinant individuals allowed us to narrow down candidate regions for the B and C loci. A cluster of SNPs most strongly associated with background colour (B locus) is found just upstream of the gene *yellow*, and a phylogenetic network for a 30 kb region around *yellow* groups individuals nearly perfectly by phenotype (Fig. 3B). Differential expression of Yellow in *Drosophila* is associated with different levels of melanism [35] and *yellow* knockouts in other butterflies show reduced melanin pigmentation [36], making this a compelling candidate for the background colour polymorphism.

Associations with forewing tip (C locus) are more dispersed across the supergene region, but the most strongly-associated SNPs are found toward the proximal end, and a phylogenetic network for this 60 kb region similarly clusters individuals by phenotype (Fig. 3B). Within this region, two of the most strongly associated SNPs fall in the gene *arrow*, which encodes a low-density lipoprotein receptor-related protein (LRP). In *Drosophila*, Arrow is essential for Wnt signalling in wing development [37]. Wnt signalling is known to underlie variation in colour pattern in *Heliconius* butterflies [38] and knock-out mutants for the Wnt ligand gene *WntA* in *D. plexippus* show a loss of pigmentation [39]. This makes *arrow* a promising candidate for the C locus gene. These putative colour patterning loci will be investigated in future studies by narrowing down the associated regions and performing functional manipulation.

Irrespective of their precise mode of action, the patterns of association imply that the B and C loci are ~1.6 Mb apart, and would therefore be fairly loosely linked under normal recombination. This physical distance translates to around 7.6 cM, assuming crossover rates similar to those in *Heliconius* [31,40], whereas the estimated recombination distance between B and C based on crosses is 1.9 cM [41]. Theory predicts that recombination suppression can be favoured if it maintains linkage disequilibrium (LD) between co-adapted alleles in the face of gene flow [1–4], but convincing empirical cases in which distinct functional loci are maintained in LD are rare [5,42]. To our knowledge, ours is the first example of a butterfly supergene in which the data strongly support the existence of two distinct genes that independently affect colour pattern maintained in LD by suppressed recombination.

It is likely that chromosomal rearrangements contribute to recombination suppression at the BC supergene. Although our short-read data do not allow us to test directly for inversions, they do reveal dramatic variation in sequencing coverage over the proximal end of the

bioRxiv preprint doi: https://doi.org/10.1101/703421; this version posted July 16, 2019. The copyright holder for this preprint (which was not certified by peer review) is the author/funder, who has granted bioRxiv a license to display the preprint in perpetuity. It is made available under aCC-BY 4.0 International license.

chromosome. Comparison of coverage among individuals suggests a large (~5 Mb) polymorphic insertion in this region (Fig. S4A). Synteny comparison with *H. melpomene* reveals that this insertion involves an expansion in copy number of a region of several hundred kb. Comparison of copy numbers for two of the genes in this insertion with several other species confirms that the insertion is derived in *D. chrysippus*, and unique to the $BC^{dorippus}$ allele (Fig. S5B, S5C). The expansion appears to occur just a few kb from the coding region of *arrow* (Fig. S4B), and is also perfectly associated with the presence of the dominant *C* phenotype (absence of black forewing tip) (Fig. S5A). It is possible that it has a causal effect on the phenotype by influencing the expression of *arrow*, but it might also be simply linked to the causative mutation. Either way, we suggest that this large structural change, which increases the length of the chromosome by nearly a third, contributes to recombination suppression between the $BC^{dorippus}$ allele and other supergene alleles by interfering with chromosome pairing in heterozygotes.

A neo-W chromosome traps a single haplotype of chromosome 15 in contact zone females

Previous crossing experiments indicated that the BC chromosome has become sex-linked in contact zone females [22]. To confirm this hypothesis using genetic tools, we created a 'cured line' by treating a female from an all-female brood with tetracycline to eliminate *Spiroplasma* and allow the survival of male offspring [23]. A cross using this female confirms perfect sex-linkage of forewing phenotype (Fig. S6A). We then used PCR assays on a subsequent sibling cross from the cured line to confirm that maternal alleles for chr15 segregate with sex while paternal alleles segregate randomly (Fig. S6B). These results exactly match the model (Fig. 1B) in which the BC supergene has become linked to the W chromosome in females, but continues to segregate as an autosome in males.

Although we were unable to definitively identify any scaffolds from the ancestral W chromosome, which is likely to be highly repetitive, we can test whether chr15 shows the expected hallmarks of a young neo-W, hypothesised to have formed through fusion to the ancestral W [22]. Due to complete absence of recombination in females, we expect that a single fused haplotype of chr15 would be spreading in the population. Any unique mutations specific to this haplotype should therefore occur at high frequency in females and be absent in males. We scanned for such high-frequency female-specific mutations, and found them to be abundant across the entire length of chr15 and nearly absent throughout the rest of the genome (Fig. 4A). At the individual level, we can clearly identify 15 females (14 collected in the contact zone and

bioRxiv preprint doi: https://doi.org/10.1101/703421; this version posted July 16, 2019. The copyright holder for this preprint (which was not certified by peer review) is the author/funder, who has granted bioRxiv a license to display the preprint in perpetuity. It is made available under aCC-BY 4.0 International license.

225 the single 'cured line' female) that consistently share these high-frequency mutations (Fig. S7).
226 Genetic distance among these females in the 'neutral' region of chr15 (outside the BC supergene)
227 is reduced, indicating that they all share a similar haplotype of the fused chromosome (Fig. 4B).

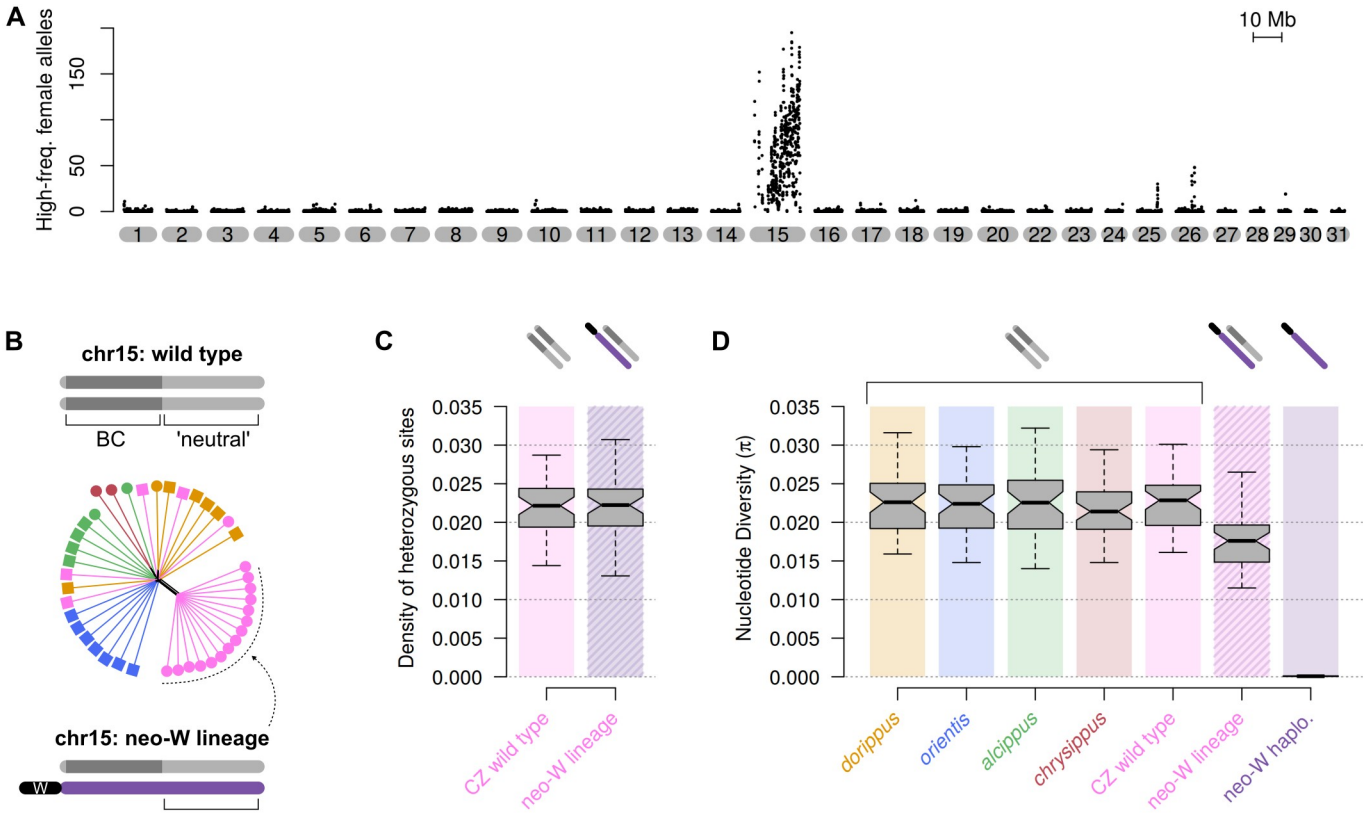

228 **Fig. 4. Recent sweep of a young neo-W.** (**A**) The number of high-frequency female-specific
229 mutations (> 20% in females and absent in males) in 100 kb sliding windows (20 kb step size).
230 **(B)** Distance-based phylogenetic network for the distal 'neutral' region of chr15 (lighter grey
231 portion), outside of the BC supergene reveals the 15 females that carry the conserved neo-W
232 haplotype. Cartoons show how the homologous neutral region of chr15 is outside of the BC
233 supergene but would still capture reduced divergence among individuals carrying a shared non-
234 recombining neo-W. (**C**) Boxplot comparing the density of heterozygous sites in 100 kb
235 windows in the neutral region of chr15 between wild type individuals from the contact zone (CZ)
236 and those carrying the neo-W. Cartoon chromosomes above the plot match those shown in panel
237 B. A relative lack of elevated heterozygosity in the neo-W lineage indicates a lack of divergence
238 of the fused neo-W haplotype, consistent with the fusion being recent. (**D**) Boxplot of nucleotide
239 diversity (π) within each population for the same neutral region of chr15. On the far right, π is
240 shown for the haploid neo-W haplotype specifically, based on partial sequences isolated from
241 this haplotype (see Methods and Fig. S8 for details). The near absence of genetic diversity
242 reflects a very rapid spread of the neo-W through the population.

bioRxiv preprint doi: https://doi.org/10.1101/703421; this version posted July 16, 2019. The copyright holder for this preprint (which was not certified by peer review) is the author/funder, who has granted bioRxiv a license to display the preprint in perpetuity. It is made available under aCC-BY 4.0 International license.

The neo-W formed recently and spread rapidly

Genetic variation accumulated in the neo-W lineage since its formation can tell us about its age. Sequence divergence between the neo-W and autosomal copies of chr15 (inferred from the density of heterozygous sites in the neutral region of chr15 in females carrying the neo-W) is not significantly different from that between the autosomal copies in 'wild type' individuals that lack the fusion (Fig. 4C, Wilcoxon signed rank test, p=0.36, n=48 100 kb windows). This implies that insufficient time has passed since the fusion event for significant accumulation of new mutations. The limited divergence of the neo-W haplotype from the autosomal copy of chr15 in each female makes it challenging to isolate. Nonetheless, by identifying diagnostic mutations that are unique to, and fixed in the neo-W linage, we were able to isolate sequencing reads from the shared haplotype and reconstruct a partial neo-W sequence for each female (Fig. S8). A dated genealogy based on these sequences places the root of the neo-W lineage at ~2200 years (26,400 generations) ago (posterior mean = 2201, std. dev. = 318).

The neo-W is present in all but one of the contact zone females, implying a rapid spread since its formation. This process is similar to a selective sweep of a beneficial mutation, except that complete recombination suppression in females means that the sweep affects the entire chromosome equally. Unlike a conventional sweep, it is not expected to eliminate genetic diversity from the population as these females will also carry an autosomal copy of chr15 inherited from their father (Fig. 1B). Indeed, we see only a 20% reduction in overall nucleotide diversity (π) on chr15 in females of the neo-W lineage (Fig. 4D). However, when we consider only the neo-W haplotype in each of these females we see a nearly complete absence of genetic variation, with a π value of 0.00007, two orders of magnitude lower than for autosomal copies of chr15 (0.0228) (Fig. 4D), further supporting a very recent and rapid spread.

The neo-W haplotype carries the recessive $BC^{chrysippus}$ allele at the BC supergene (Fig. S3). However, many of the individuals carrying the neo-W express the *dorippus* phenotype because they carry the dominant $BC^{dorippus}$ allele on their autosomal chr15 chromatid. This highlights the question of what selective driver might have caused the spread of a recessive colour patterning allele.

bioRxiv preprint doi: https://doi.org/10.1101/703421; this version posted July 16, 2019. The copyright holder for this preprint (which was not certified by peer review) is the author/funder, who has granted bioRxiv a license to display the preprint in perpetuity. It is made available under aCC-BY 4.0 International license.

Hitchhiking between the neo-W and *Spiroplama*

We hypothesised that the neo-W has spread not due to direct natural selection on warning pattern but rather through co-inheritance with the male-killing *Spiroplasma*, which is itself spreading through the population as a selfish element. Experiments have shown that infected female offspring may show increased survival relative to those from uninfected broods due to reduced competition for resources [43]. For this to drive the spread of the neo-W would require strict vertical inheritance of *Spiroplasma* down the female line, such that it is always co-inherited with the neo-W.

We identified nine scaffolds making up the 1.75 Mb *Spiroplasma* genome in our *D. chrysippus* assembly (Fig. S9A). Infected individuals are clearly identifiable by mapping resequencing reads to the *Spiroplasma* scaffolds (Fig. S9B). As predicted, all females in the neo-W lineage are infected (with the exception of the cured line female, in which *Spiroplasma* had been eliminated). Moreover, all infected females fall into the same mitochondrial clade (Fig. 5A). To confirm that the *Spiroplasma* is strictly vertically inherited and always associated with a single female lineage, we used PCR assays for *Spiroplasma* and mitochondrial haplotype and expanded our sample size to 158 individuals, including samples used in previous studies going back two decades [19,23] (Data S1, Fig. S10). This confirms the perfect association: 100% of infected individuals (n=42) carry the same mitochondrial haplotype, and this haplotype is otherwise rare, occurring in 8% of uninfected individuals (n=116) (Fig. S10).

Like the neo-W, the *Spiroplasma* genomes carry limited variation among individuals (π = 0.0005), consistent with a single and recent outbreak of the endosymbiont. Although the lack of variation makes it challenging to infer genealogies, our inferred maximum likelihood genealogies for the neo-W and *Spiroplasma* are strikingly congruent (Fig 4B). In a permutation test for congruence [44] the observed level exceeds all 100,000 random permutations, indicating strong support for co-inheritance of the neo-W and *Spiroplasma* [45].

bioRxiv preprint doi: https://doi.org/10.1101/703421; this version posted July 16, 2019. The copyright holder for this preprint (which was not certified by peer review) is the author/funder, who has granted bioRxiv a license to display the preprint in perpetuity. It is made available under aCC-BY 4.0 International license.

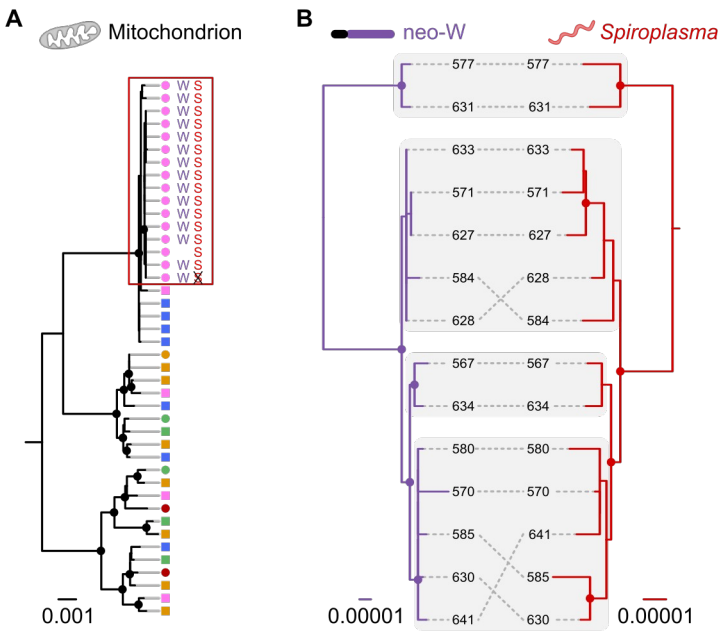

Fig. 5. Matrilineal inheritance causes coupling between neo-W and *Spiroplasma*. (**A**) Maximum likelihood phylogeny for the whole mitochondrial genome. Individuals are coloured according to population of origin (see Fig. 1A), and those carrying the neo-W ('W') and *Spiroplasma* ('S') are indicated (including one cured individual in which *Spiroplasma* was eliminated). Females are indicated by circles and males by squares. (**B**) Maximum likelihood phylogenies for the neo-W haplotype and *Spiroplasma* genome isolated from infected females. Corresponding clades are shaded to indicate congruence. Note that two samples are excluded in panel B: the cured sample which lacked *Spiroplasma* due to tetracycline treatment, and one infected female found to lack the neo-W. Whether the latter represents an ancestral state or secondary loss requires further investigation. In all trees, nodes supported by more than 700 of 1000 bootstrap replicates are indicated by circles.

The combined spread of three unlinked DNA molecules – the mitochondrial genome, neo-W and *Spiroplasma* genome – constitutes a form of genetic hitchhiking, but is facilitated by their strict matrilineal inheritance rather than physical linkage. While it is well known that selfish maternally-inherited endosymbionts can drive the spread of a single mitochondrial haplotype through a population and even across species boundaries [46,47], our findings show how an entire chromosome can be captured in the same way. Hitchhiking with selfish elements may be of general importance in driving the spread of neo-sex chromosomes.

In *D. chrysippus*, it is currently unclear whether the neo-W or male-killer emerged first. It is also unclear whether their co-occurrence in a single ancestor was simply a coincidence or

bioRxiv preprint doi: https://doi.org/10.1101/703421; this version posted July 16, 2019. The copyright holder for this preprint (which was not certified by peer review) is the author/funder, who has granted bioRxiv a license to display the preprint in perpetuity. It is made available under aCC-BY 4.0 International license.

instead reflects some functional connection, such as the suggestion that the neo-W might confer susceptibility to the male killer [22]. It is important to note that this is not the first time a neo-sex chromosome has formed in this taxon. A fusion of chromosome 21 to the ancestral Z chromosome occurred in an ancestor of all *Danaus* species, producing a neo-Z [9,32,48]. It is speculated that a fusion of chromosome 21 to the ancestral W also occurred [9,48] but this is difficult to conclusively verify due to degradation of W chromosome over longer timescales. If this hypothesis of an ancient neo-W is correct, then the neo-W we describe (W-chr15) might in fact be better described as a neo-neo-W (W-chr21-chr15). It is possible that the spread of the original W-chr21 was also driven by hitchhiking with a selfish endosymbiont.

Genetic and phenotypic consequences of recombination suppression

Sex chromosome evolution in many other taxa involves the progressive spread of recombination suppression outward from the a sex-determining locus [49]. By contrast, the absence of crossing over in female meiosis means that a lepidopteran neo-W experiences complete and immediate recombination suppression over its entire length. The young age of the *D. chrysippus* neo-W therefore provides a rare opportunity to study the early evolutionary consequences of recombination suppression across an entire chromosome. Two related processes could shape its evolution: hitchhiking of pre-existing deleterious mutations that were initially rare in the population [6], and accumulation of novel deleterious mutations due to reduced purging through recombination and selection (i.e. Muller's Ratchet) [7].

As a proxy for the 'genetic load' of deleterious mutations in the population, we considered P_n/P_s, the ratio of non-synonymous to synonymous polymorphisms. Due to purifying selection, non-synonymous polymorphisms are typically rare, and where they do occur the mutant allele typically occurs at low frequency in the population [50]. When considering all polymorphisms in the neo-W lineage, we see no overall excess of P_n/P_s for chr15 (excluding genes within the BC supergene excluded to avoid bias) (Fig. S11A). However, when we partition polymorphisms by allele frequency, we see a two 2-3 fold increase in P_n/P_s for mutations at high frequency, specifically those at exactly 50% frequency, on chr15 (Fig. S11B, S11C). This implies that hitchhiking has indeed led to the inadvertent spread of pre-existing deleterious alleles that were initially rare in the population but happened to be present on the neo-W haplotype, and are therefore now found in all females in this lineage. The lack of an overall excess of genetic load

bioRxiv preprint doi: https://doi.org/10.1101/703421; this version posted July 16, 2019. The copyright holder for this preprint (which was not certified by peer review) is the author/funder, who has granted bioRxiv a license to display the preprint in perpetuity. It is made available under aCC-BY 4.0 International license.

probably reflects insufficient time for accumulation of new deleterious mutations since the formation of the neo-W.

At the phenotypic level, perhaps counter-intuitively, the spread of a single supergene allele on the neo-W has not caused homogenization of warning pattern among contact zone females, and might in fact have the opposite effect. In locations where the neo-W and *Spiroplasma* are nearly fixed, such as our sampling site near Nairobi, the high incidence of male killing implies that the population is strongly shaped by immigrant males. Since the $BC^{chrysippus}$ allele on the neo-W is universally recessive, daughters will tend to match the phenotype of their immigrant father. However, because the neo-W is always transmitted to daughters, the paternal chr15 copy will be lost to male killing after one generation, creating a genetic sink for immigrant male genes [22] (Fig. S12B). This combination of processes makes for a female population that is highly sensitive to the source of immigrants, which is known to fluctuate seasonally with monsoon winds [16,51] (Fig. S12A). This model leads to the testable prediction that seasonal fluctuations in female phenotypes should be most dramatic where male killing is most abundant.

Future evolutionary trajectories

The future of the neo-W and *Spiroplasma* outbreak is uncertain. A lack of males could lead to local extinctions [27], but extinction of the entire infected lineage is unlikely given the high dispersal ability of males. Since the spread of the male killer is dependent on reduced sibling competition in all-female broods, the spread might also be limited in environments where competition is reduced, or where oviposition behaviour reduces opportunities for competition [43]. In other systems, sex-ratio distortion has driven adaptive responses by the host, including changes to the mating system [52] and the evolution of resistance to male-killing [53,54]. The absence of evidence for these phenomena in *D. chrysippus* might simply reflect the recency of the male killing outbreak. Eventually, we also expect the non-recombining neo-W to begin to degenerate through further hitchhiking, gene loss and the spread of repetitive elements [8,49]. This young system provides a rare opportunity to study how these phenomena unfold through time and space.

bioRxiv preprint doi: https://doi.org/10.1101/703421; this version posted July 16, 2019. The copyright holder for this preprint (which was not certified by peer review) is the author/funder, who has granted bioRxiv a license to display the preprint in perpetuity. It is made available under aCC-BY 4.0 International license.

Methods

Reference genome sequencing, assembly and annotation

Detailed methods for generation of the *D. chrysippus* reference genome are provided in Supplementary Methods. Briefly, a draft assembly was generated using SPAdes [55] from a combination of paired-end and mate-pair libraries of various insert sizes. Scaffolding and resolution of haplotypes was performed using Redundans [56] and Haplomerger2 [57]. The assembly was annotated using a combination of de-novo gene predictors yielding 16,654 protein coding genes. Mitochondrial genomes were assembled using NOVOplasty [58].

Although we currently lack linkage information for further scaffolding, we generated a pseudo-chromosomal assembly based on homology with the highly contiguous *Heliconius melpomene* genome [30,31,59], adjusted for known karyotypic differences [9,30–32,48]. In total, 282 Mb (87% of the genome) could be confidently assigned to chromosomes (Fig. S1).

Scaffolds representing the *Spiroplasma* genome were identified based on read depth of re-mapped reads (Fig. S9A) and homology to other available *Spirolasma* genomes. Annotation was performed using the RAST server pipeline [60,61].

Population sample resequencing and genotyping

This study made use of 42 newly sequenced *D. chrysippus* individuals, as well as previously sequenced individuals of the sister species, *D. petilia* (n=1), and next closest outgroup *D. gilippus* (n=2) [62] (Table S9). Details of DNA extraction, sequencing and genotyping are provided in Supplementary Methods. Briefly, DNA was extracted from thorax tissue and sequenced (paired-end, 150 bp) to a mean depth of coverage 20x or greater. Reads were mapped to the *D. chrysippus* reference assembly using Stampy [63] v1.0.31 and genotyping was performed using GATK version 3 [64,65]. Genotype calls were required to have an individual read depth ≥ 8, and heterozygous and alternate allele calls were further required to have an individual genotype quality (GQ) ≥ 20 for downstream analyses.

Genomic differentiation and associations with wing pattern

We used the fixation index (F_{ST}) to examine genetic differentiation across the genome among the three subspecies for which we had six or more individuals sequenced. F_{ST} was computed using the script popgenWindows.py (github.com/simonhmartin/genomics_general)

bioRxiv preprint doi: https://doi.org/10.1101/703421; this version posted July 16, 2019. The copyright holder for this preprint (which was not certified by peer review) is the author/funder, who has granted bioRxiv a license to display the preprint in perpetuity. It is made available under aCC-BY 4.0 International license.

with a sliding windows of 100 kb, stepping in increments of 20 kb. Windows with fewer than 20,000 genotyped sites after filtering (see above) were ignored.

To identify SNPs associated with the three Mendelian colour pattern traits (i.e. the A B and C loci) (Fig. 1A), we used PLINK v1.9 [66] with the '--assoc' option, and provided quantitative phenotypes of 0, 1 or 0.5 for assumed heterozygotes. In addition to the quality and depth filters above, SNPs used for this analysis were required to have genotypes for at least 40 individuals, a minor allele count of at least 2, and to be heterozygous in no more than 75% of individuals. SNPs were also thinned to a minimum distance of 100 bp.

To examine relationships among diploid individuals in specific regions of interest, we constructed phylogenetic networks using the Neighbor-Net [67] algorithm, implemented in SplitsTree [68]. Pairwise distances used for input were computed using the script distMat.py (github.com/simonhmartin/genomics_general).

Haplotype cluster assignment

To assign haplotypes to clusters in the BC supergene region, we first phased genotypes using SHAPEIT2 [69,70] using SNPs filtered as for association analysis above, except with a minor allele count of at least 4, and no thinning. Default parameters were used for phasing except that the effective population size was set to $3x10^6$. To minimise phasing switch errors, we analysed each 20 kb window separately. Cluster assignment for both haplotypes from each individual was based on average genetic distance to all haplotypes from each of three reference groups: *D. c. dorippus*, *D. c. orientis*, or *D. c. alcippus* (which is representative of *chrysippus* as they share the same alleles at the BC supergene). A haplotype was assigned to one of the three groups if its average genetic distance to members of that group was less than 80% the average distance to the other two groups, otherwise it was left as unassigned. Genetic distances were computed using the script popgenWindows.py (github.com/simonhmartin/genomics_general).

Identification of neo-W specific sequencing reads

To identify females carrying the neo-W chromosome, we visualised the distribution of female-specific derived mutations that occur at high-frequency. Allele frequencies were computed using the script freq.py (github.com/simonhmartin/genomics_general). Due to the absence of female meiotic crossing over in Lepidoptera, all females carrying the neo-W fusion should share a conserved chromosomal haplotype for the entire fused chromosome. To isolate

bioRxiv preprint doi: https://doi.org/10.1101/703421; this version posted July 16, 2019. The copyright holder for this preprint (which was not certified by peer review) is the author/funder, who has granted bioRxiv a license to display the preprint in perpetuity. It is made available under aCC-BY 4.0 International license.

this shared fused haplotype from the autosomal copy, we first identified diagnostic mutations as those that are present in a single copy in each member of the 'neo-W lineage' and absent from all other individuals and outgroups. We then isolated the sequencing read pairs from each of these females that carry the derived mutation (Fig. S8). This resulted in a patchy alignment file, with a stack of read pairs over each diagnostic mutation. Based on these aligned reads, we genotyped each individuals as described above, except here setting the ploidy level to 1, and requiring a minimum read depth of 3.

Diversity and divergence of the neo-W

The lack of recombination across the neo-W makes it possible to gain insights into its age. Over time, mutations will arise that differentiate the neo-W from the recombining autosomal copies of the chromosome. We estimated this divergence based on average heterozygosity in females carrying the neo-W, and compared it to heterozygosity from contact-zone individuals not carrying the neo-W. Heterozygosity was computed using the Python script popgenWindows.py (github.com/simonhmartin/genomics_general) focusing only on the 'neutral' portion of the chromosome (i.e. the distal portion from 11 Mb onwards), which is outside of the BC supergene. Heterozygosity was computed in 100 kb windows, and windows were discarded if they contained fewer than 20,000 sites genotyped in at least two individuals from each population.

A recent spread of the neo-W through the population should also be detectable in the form of strong conservation of the neo-W haplotype in all females that carry it (i.e. reduced genetic diversity). We therefore computed nucleotide diversity (π) in 100 kb windows as above. Reported values of π and heterozygosity represent the mean +- standard deviation across 100 kb windows.

Genealogical analyses

We produced maximum likelihood trees for the mitochondrial genome, neo-W and *Spiroplasma* genome, using PhyML v3 [71] with the GTR substitution model. Given the small number of SNPs in both the neo-W and *Spiroplasma* genome, regions with inconsistent coverage across individuals were excluded manually. Only sites with no missing genotypes were included.

We estimated the root node age for the neo-W using BEAST2 [72,73] version 2.5.1 with a fixed clock model and an exponential population growth prior. For all other priors we used the

bioRxiv preprint doi: https://doi.org/10.1101/703421; this version posted July 16, 2019. The copyright holder for this preprint (which was not certified by peer review) is the author/funder, who has granted bioRxiv a license to display the preprint in perpetuity. It is made available under aCC-BY 4.0 International license.

462 defaults as defined by BEAUti v2.5.1. We assumed a mutation rate of 2.9×10^{-9} per generation
463 based on a direct estimate for *Heliconius* butterflies [74] and 12 generations per year [75].
464 BEAST2 was run for 500,000,000 iterations, sampling every 50,000 generations, and we used
465 Tracer [76] version 1.7.1 to check for convergence of posterior distributions and compute the
466 root age after discarding a burn-in of 10%.

467 We tested for congruence between the neo-W and *Spiroplasma* trees using PACo [44],
468 which assesses the goodness-of-fit between host and parasite distance matrices, with 100,000
469 permutations. Distance matrices were computed using the script distMat.py
470 (github.com/simonhmartin/genomics_general).

471 **Analysis of synonymous and non-synonymous polymorphism**

472 We computed P_n/P_s as as the ratio of non-synonymous polymorphisms per non-
473 synonymous site to synonymous polymorphisms per synonymous site. Synonymous and non-
474 synonymous sites were defined conservatively as 4-fold degenerate and 0-fold degenerate codon
475 positions, respectively, with the requirement that the other two codon positions are invariant
476 across the entire dataset. Only sites genotyped in all 15 females in the neo-W lineage were
477 considered, and counts were stratified by minor allele frequency using the script sfs.py
478 (github.com/simonhmartin/genomics_general).

479 **Butterfly rearing and molecular diagnostics**

480 To generate a stock line that is cured of *Spiroplasma* infection, we treated caterpillars from
481 all-female broods with Tetracycline, following Jiggins et al. [23]. A 'cured line' was initiated
482 from a single treated female that had the heterozygous *Cc* '*transiens*' phenotype (Fig 1A). This
483 female was crossed to a wild male (homozygous *cc*) to test for sex linkage of phenotype. The
484 cured line was using sibling crosses and the persistence of males indicated that spiroplasma had
485 been eliminated.

486 We then applied a molecular test for sex linkage of chr15 using the F5 brood from the
487 cured line. We designed two separate PCR diagnostics based on SNPs segregating on chr15 to
488 distinguish between the two chromosomes of the male and the female parents (Table S10). PCR
489 was performed using the Phusion HF Master Mix and HF Buffer (New England Biosciences).

490 To screen for *Spiroplasma* infection, we designed a PCR assay targeting the
491 glycerophosphoryl diester phosphodiesterase (GDP) gene (Table S10). PCR was performed as

bioRxiv preprint doi: https://doi.org/10.1101/703421; this version posted July 16, 2019. The copyright holder for this preprint (which was not certified by peer review) is the author/funder, who has granted bioRxiv a license to display the preprint in perpetuity. It is made available under aCC-BY 4.0 International license.

above. We confirmed the the sensitivity of this diagnostic by analyzing individuals of known infection status based on whole genome sequencing.

To investigate whether *Spiroplasma* infection was always associated with a single mitochondrial haplotype, we designed a PCR RFLP for the Cytochrome Oxidase Subunit I (COI) that differentiates the infected 'K' lineage from uninfected (Table S10). PCR was performed as above. A subset of products were verified by Sanger sequencing after purification using the QIAquick PCR Purification Kit (Qiagen, USA).

References

1. Kirkpatrick M, Barton N. Chromosome inversions, local adaptation and speciation. Genetics. 2006;173: 419–34. doi:10.1534/genetics.105.047985

2. Bürger R, Akerman A. The effects of linkage and gene flow on local adaptation: A two-locus continent–island model. Theor Popul Biol. Academic Press; 2011;80: 272–288. doi:10.1016/J.TPB.2011.07.002

3. Guerrero RF, Rousset F, Kirkpatrick M. Coalescent patterns for chromosomal inversions in divergent populations. Philos Trans R Soc B Biol Sci. 2012;367: 430–438. doi:10.1098/rstb.2011.0246

4. Charlesworth D, Charlesworth B. Selection on recombination in clines. Genetics. 1979;91: 575–580.

5. Charlesworth D. The status of supergenes in the 21st century: Recombination suppression in Batesian mimicry and sex chromosomes and other complex adaptations. Evol Appl. John Wiley & Sons, Ltd (10.1111); 2016;9: 74–90. doi:10.1111/eva.12291

6. Rice WR. Genetic hitchhiking and the evolution of reduced genetic activity of the Y sex chromosome. Genetics. 1987;116: 161–167.

7. Charlesworth B. Model for evolution of Y chromosomes and dosage compensation. Proc Natl Acad Sci U S A. 1978;75: 5618–22.

8. Bachtrog D, Charlesworth B. The temporal dynamics of processes underlying Y chromosome degeneration. Genetics. Genetics; 2008;179: 1513–25. doi:10.1534/genetics.107.084012

9. Mongue AJ, Nguyen P, Volenikova A, Walters JR. Neo-sex chromosomes in the Monarch butterfly, Danaus plexippus. bioRxiv. 2017; doi:10.1534/g3.117.300187

bioRxiv preprint doi: https://doi.org/10.1101/703421; this version posted July 16, 2019. The copyright holder for this preprint (which was not certified by peer review) is the author/funder, who has granted bioRxiv a license to display the preprint in perpetuity. It is made available under aCC-BY 4.0 International license.

10. Bracewell RR, Bentz BJ, Sullivan BT, Good JM. Rapid neo-sex chromosome evolution and incipient speciation in a major forest pest. Nat Commun. Springer US; 2017;8. doi:10.1038/s41467-017-01761-4

11. Pala I, Naurin S, Stervander M, Hasselquist D, Bensch S, Hansson B. Evidence of a neo-sex chromosome in birds. Heredity. Nature Publishing Group; 2012;108: 264–272. doi:10.1038/hdy.2011.70

12. Kitano J, Ross JA, Mori S, Kume M, Jones FC, Chan YF, et al. A role for a neo-sex chromosome in stickleback speciation. Nature. Nature Publishing Group; 2009;461: 1079–1083. doi:10.1038/nature08441

13. Nguyen P, Sykorova M, Sichova J, Kuta V, Dalikova M, Capkova Frydrychova R, et al. Neo-sex chromosomes and adaptive potential in tortricid pests. Proc Natl Acad Sci. 2013;110: 6931–6936. doi:10.1073/pnas.1220372110

14. Carabajal Paladino LZ, Provazníková I, Berger M, Bass C, Aratchige NS, López SN, et al. Sex Chromosome Turnover in Moths of the Diverse Superfamily Gelechioidea. Barluenga M, editor. Genome Biol Evol. Narnia; 2019;11: 1307–1319. doi:10.1093/gbe/evz075

15. Steinemann M, Steinemann S. Enigma of Y chromosome degeneration: neo-Y and neo-X chromosomes of Drosophila miranda a model for sex chromosome evolution. Genetica. 1998;102–103: 409–20.

16. Smith DAS, Owen DF, Gordon IJ, Lowis NK. The butterfly Danaus chrysippus (L .) in East Afiica : polymorphism and morph-ratio clines within a complex , extensive and dynamic hybrid zone. Zool J Linn Soc. 1997;120: 51–78.

17. Smith DAS. Heterosis, epistasis and linkage disequilibrium in a wild population of the polymorphic butterfly Danaus chrysippus (L .). Zool J Linn Soc. 1980;69: 87–109.

18. Smith D a S, Owen DF, Gordon IJ, Owiny AM. Polymorphism and evolution in the butterfly Danaus chrysippus (L.) (Lepidoptera: Danainae). Heredity. 1993;71: 242–251. doi:10.1038/hdy.1993.132

19. Smith DAS, Gordon IJ, Allen JA. Reinforcement in hybrids among once isolated semispecies of Danaus chrysippus (L.) and evidence for sex chromosome evolution. Ecol Entomol. 2010;35: 77–89. doi:10.1111/j.1365-2311.2009.01143.x

20. Smith DAS. Genetics of Some Polymorphic Forms of the African Butterfly Danaus chrysippus L. (Lepidoptera: Danaidae). Insect Syst Evol. Brill; 1975;6: 134–144. doi:10.1163/187631275X00235

21. Clarke CA, Sheppard PM, Smith AG. genetics of fore and hindwing colour in crosses between Danaus chrysippus from Australia and from Sierra Leone (Danaidae). Lepid Soc J. 1973;

bioRxiv preprint doi: https://doi.org/10.1101/703421; this version posted July 16, 2019. The copyright holder for this preprint (which was not certified by peer review) is the author/funder, who has granted bioRxiv a license to display the preprint in perpetuity. It is made available under aCC-BY 4.0 International license.

22. Smith DAS, Gordon IJ, Traut W, Herren J, Collins S, Martins DJ, et al. A neo-W chromosome in a tropical butterfly links colour pattern, male-killing, and speciation. Proc R Soc B Biol Sci. 2016;283: 20160821. doi:10.1098/rspb.2016.0821

23. Jiggins FM, Hurst GD, Jiggins CD, v d Schulenburg JH, Majerus ME. The butterfly Danaus chrysippus is infected by a male-killing Spiroplasma bacterium. Parasitology. 2000;120 (Pt 5: 439–46. doi:10.1017/S0031182099005867

24. Herren JK, Gordon I, Holland PWH, Smith D. The butterfly Danaus chrysippus (Lepidoptera: Nymphalidae) in Kenya is variably infected with respect to genotype and body size by a maternally transmitted male-killing endosymbiont (Spiroplasma). Int J Trop Insect Sci. 2007;27: 62. doi:10.1017/S1742758407818327

25. Gordon IJ, Ireri P, Smith DAS. Hologenomic speciation: Synergy between a male-killing bacterium and sex-linkage creates a “magic trait” in a butterfly hybrid zone. Biol J Linn Soc. 2014;111: 92–109. doi:10.1111/bij.12185

26. Lushai G, Allen JA, Goulson D, Maclean N, Smith DAS. The butterfly Danaus chrysippus (L.) in East Africa comprises polyphyletic, sympatric lineages that are, despite behavioural isolation, driven to hybridization by female-biased sex ratios. Biol J Linn Soc. 2005;86: 117–131. doi:10.1111/j.1095-8312.2005.00526.x

27. Idris E, Saeed M. Hassan S. Biased sex ratios and aposematic polymorphism in African butterflies: A hypothesis. Ideas Ecol Evol. 2013;6: 5–16. doi:10.4033/iee.2013.6.2.n

28. Simão FA, Waterhouse RM, Ioannidis P, Kriventseva E V., Zdobnov EM. BUSCO: assessing genome assembly and annotation completeness with single-copy orthologs. Bioinformatics. Oxford University Press; 2015;31: 3210–3212. doi:10.1093/bioinformatics/btv351

29. Heliconius Genome Consortium T. Butterfly genome reveals promiscuous exchange of mimicry adaptations among species. Nature. 2012;487: 94–8. doi:10.1038/nature11041

30. Davey JW, Chouteau M, Barker SL, Maroja L, Baxter SW, Simpson F, et al. Major Improvements to the Heliconius melpomene Genome Assembly Used to Confirm 10 Chromosome Fusion Events in 6 Million Years of Butterfly Evolution. G3. 2016;6: 695–708. doi:10.1534/g3.115.023655

31. Davey JW, Barker SL, Rastas PM, Pinharanda A, Martin SH, Durbin R, et al. No evidence for maintenance of a sympatric Heliconius species barrier by chromosomal inversions. Evol Lett. 2017;1: 138–154. doi:10.1002/evl3.12

32. Ahola V, Lehtonen R, Somervuo P, Salmela L, Koskinen P, Rastas P, et al. The Glanville fritillary genome retains an ancient karyotype and reveals selective chromosomal fusions in Lepidoptera. Nat Commun. 2014;5: 1–9. doi:10.1038/ncomms5737

bioRxiv preprint doi: https://doi.org/10.1101/703421; this version posted July 16, 2019. The copyright holder for this preprint (which was not certified by peer review) is the author/funder, who has granted bioRxiv a license to display the preprint in perpetuity. It is made available under aCC-BY 4.0 International license.

33. Leffler EM, Bullaughey K, Matute DR, Meyer WK, Ségurel L, Venkat A, et al. Revisiting an old riddle: what determines genetic diversity levels within species? PLoS Biol. 2012;10: e1001388. doi:10.1371/journal.pbio.1001388

34. Martin SH, Dasmahapatra KK, Nadeau NJ, Salazar C, Walters JR, Simpson F, et al. Genome-wide evidence for speciation with gene flow in Heliconius butterflies. Genome Res. 2013;23: 1817–1828. doi:10.1101/gr.159426.113

35. Wittkopp PJ, Vaccaro K, Carroll SB. Evolution of yellow Gene Regulation and Pigmentation in Drosophila. Curr Biol. Cell Press; 2002;12: 1547–1556. doi:10.1016/S0960-9822(02)01113-2

36. Zhang L, Martin A, Perry MW, van der Burg KRL, Matsuoka Y, Monteiro A, et al. Genetic Basis of Melanin Pigmentation in Butterfly Wings. Genetics. Genetics; 2017;205: 1537–1550. doi:10.1534/genetics.116.196451

37. Rives AF, Rochlin KM, Wehrli M, Schwartz SL, DiNardo S. Endocytic trafficking of Wingless and its receptors, Arrow and DFrizzled-2, in the Drosophila wing. Dev Biol. Academic Press; 2006;293: 268–283. doi:10.1016/j.ydbio.2006.02.006

38. Martin A, Papa R, Nadeau NJ, Hill RI, Counterman BA, Halder G. Diversification of complex butterfly wing patterns by repeated regulatory evolution of a Wnt ligand. Proc Natl Acad Sci U S A. 2012;109: 12632–12637. doi:doi.org/10.1073/pnas.1204800109

39. Mazo-Vargas A, Concha C, Livraghi L, Massardo D, Wallbank RWR, Zhang L, et al. Macroevolutionary shifts of WntA function potentiate butterfly wing-pattern diversity. Proc Natl Acad Sci. 2017;114: 10701 LP – 10706.

40. Van Belleghem SM, Rastas P, Papanicolaou A, Martin SH, Arias CF, Supple MA, et al. Complex modular architecture around a simple toolkit of wing pattern genes. Nat Ecol Evol. 2017;1: 0052. doi:10.1038/s41559-016-0052

41. Smith DAS. Evidence for autosomal meiotic drive in the butterfly Danaus chrysippus L. Heredity. 1976;36: 139–142.

42. Coughlan JM, Willis JH. Dissecting the role of a large chromosomal inversion in life history divergence throughout the *Mimulus guttatus* species complex. Mol Ecol. John Wiley & Sons, Ltd (10.1111); 2019;28: 1343–1357. doi:10.1111/mec.14804

43. Gordon IJ, Ireri P, Smith DAS. Preference for isolated host plants facilitates invasion of Danaus chrysippus (Linnaeus, 1758) (Lepidoptera: Nymphalidae) by a bacterial male-killer Spiroplasma. Austral Entomol. 2015;54: 210–216. doi:10.1111/aen.12113

44. Balbuena JA, Míguez-Lozano R, Blasco-Costa I. PACo: A Novel Procrustes Application to Cophylogenetic Analysis. Moreau CS, editor. PLoS One. Public Library of Science; 2013;8: e61048. doi:10.1371/journal.pone.0061048

bioRxiv preprint doi: https://doi.org/10.1101/703421; this version posted July 16, 2019. The copyright holder for this preprint (which was not certified by peer review) is the author/funder, who has granted bioRxiv a license to display the preprint in perpetuity. It is made available under aCC-BY 4.0 International license.

45. Richardson MF, Weinert LA, Welch JJ, Linheiro RS, Magwire MM, Jiggins FM, et al. Population Genomics of the Wolbachia Endosymbiont in Drosophila melanogaster. PLoS Genet. 2012;8. doi:10.1371/journal.pgen.1003129

46. Jiggins FM. Male-killing Wolbachia and mitochondrial DNA: selective sweeps, hybrid introgression and parasite population dynamics. Genetics. 2003;164: 5–12.

47. Hurst GDD, Jiggins FM. Problems with mitochondrial DNA as a marker in population, phylogeographic and phylogenetic studies: The effects of inherited symbionts. Proc R Soc B Biol Sci. 2005;272: 1525–1534. doi:10.1098/rspb.2005.3056

48. Traut W, Ahola V, Smith DAS, Gordon IJ, Ffrench-Constant RH. Karyotypes versus Genomes: The Nymphalid Butterflies Melitaea cinxia, Danaus plexippus, and D. chrysippus. Cytogenet Genome Res. 2018;153: 46–53. doi:10.1159/000484032

49. Wright AE, Dean R, Zimmer F, Mank JE. How to make a sex chromosome. Nature Communications. Nature Publishing Group; 2016. p. 12087. doi:10.1038/ncomms12087

50. Fay JC, Wyckoff GJ, Wu C-I. Positive and Negative Selection on the Human Genome. Genetics. 2001;158: 1227–1234.

51. Smith DAS, Owen DF. Colour genes as markers for migratory activity: The butterfly Danaus chrysippus in Africa. Oikos. 1997;78: 127–135.

52. Jiggins FM, Hurst GDD, Majerus MEN. Sex-ratio-distorting Wolbachia causes sex-role reversal in its butterfly host. Proc R Soc B Biol Sci. 2000;267: 69–73. doi:10.1098/rspb.2000.0968

53. Hornett EA, Charlat S, Duplouy AMR, Davies N, Roderick GK, Wedell N, et al. Evolution of male-killer suppression in a natural population. PLoS Biol. 2006;4: 1643–1648. doi:10.1371/journal.pbio.0040283

54. Wilfert L, Jiggins FM. The dynamics of reciprocal selective sweeps of host resistance and a parasite counter-adaptation in Drosophila. Evolution. Wiley/Blackwell (10.1111); 2013;67: 761–773. doi:10.1111/j.1558-5646.2012.01832.x

55. Bankevich A, Nurk S, Antipov D, Gurevich AA, Dvorkin M, Kulikov AS, et al. SPAdes: A New Genome Assembly Algorithm and Its Applications to Single-Cell Sequencing. J Comput Biol. Mary Ann Liebert, Inc. 140 Huguenot Street, 3rd Floor New Rochelle, NY 10801 USA ; 2012;19: 455–477. doi:10.1089/cmb.2012.0021

56. Pryszcz LP, Gabaldón T. Redundans: an assembly pipeline for highly heterozygous genomes. Nucleic Acids Res. Oxford University Press; 2016;44: e113–e113. doi:10.1093/nar/gkw294

bioRxiv preprint doi: https://doi.org/10.1101/703421; this version posted July 16, 2019. The copyright holder for this preprint (which was not certified by peer review) is the author/funder, who has granted bioRxiv a license to display the preprint in perpetuity. It is made available under aCC-BY 4.0 International license.

57. Huang S, Kang M, Xu A. HaploMerger2: rebuilding both haploid sub-assemblies from high-heterozygosity diploid genome assembly. Berger B, editor. Bioinformatics. Oxford University Press; 2017;33: 2577–2579. doi:10.1093/bioinformatics/btx220

58. Dierckxsens N, Mardulyn P, Smits G. NOVOPlasty: *de novo* assembly of organelle genomes from whole genome data. Nucleic Acids Res. Oxford University Press; 2016;45: gkw955. doi:10.1093/nar/gkw955

59. Dasmahapatra KK, Walters JR, Briscoe AD, Davey JW, Whibley A, Nadeau NJ, et al. Butterfly genome reveals promiscuous exchange of mimicry adaptations among species. Nature. Nature Publishing Group; 2012;487: 94–8. doi:10.1038/nature11041

60. Overbeek R, Olson R, Pusch GD, Olsen GJ, Davis JJ, Disz T, et al. The SEED and the Rapid Annotation of microbial genomes using Subsystems Technology (RAST). Nucleic Acids Res. Oxford University Press; 2014;42: D206–D214. doi:10.1093/nar/gkt1226

61. Aziz RK, Bartels D, Best AA, DeJongh M, Disz T, Edwards RA, et al. The RAST Server: Rapid Annotations using Subsystems Technology. BMC Genomics. BioMed Central; 2008;9: 75. doi:10.1186/1471-2164-9-75

62. Zhan S, Zhang W, Niitepõld K, Hsu J, Haeger JF, Zalucki MP, et al. The genetics of monarch butterfly migration and warning colouration. Nature. 2014;514: 317–21. doi:10.1038/nature13812

63. Lunter G, Goodson M. Stampy: a statistical algorithm for sensitive and fast mapping of Illumina sequence reads. Genome Res. 2011;21: 936–9. doi:10.1101/gr.111120.110

64. DePristo M a, Banks E, Poplin R, Garimella K V, Maguire JR, Hartl C, et al. A framework for variation discovery and genotyping using next-generation DNA sequencing data. Nat Genet. 2011;43: 491–8. doi:10.1038/ng.806

65. Van der Auwera GA, Carneiro MO, Hartl C, Poplin R, del Angel G, Levy-Moonshine A, et al. From fastQ data to high-confidence variant calls: The genome analysis toolkit best practices pipeline. Curr Protoc Bioinforma. Hoboken, NJ, USA: John Wiley & Sons, Inc.; 2013;43: 11.10.1-11.10.33. doi:10.1002/0471250953.bi1110s43

66. Chang CC, Chow CC, Tellier LC, Vattikuti S, Purcell SM, Lee JJ. Second-generation PLINK: rising to the challenge of larger and richer datasets. Gigascience. Narnia; 2015;4: 7. doi:10.1186/s13742-015-0047-8

67. Bryant D, Moulton V. Neighbor-Net: An Agglomerative Method for the Construction of Phylogenetic Networks. Mol Biol Evol. 2003;21: 255–265. doi:10.1093/molbev/msh018

68. Huson DH, Bryant D. Application of Phylogenetic Networks in Evolutionary Studies. Mol Biol Evol. 2006;23: 254–267. doi:10.1093/molbev/msj030

bioRxiv preprint doi: https://doi.org/10.1101/703421; this version posted July 16, 2019. The copyright holder for this preprint (which was not certified by peer review) is the author/funder, who has granted bioRxiv a license to display the preprint in perpetuity. It is made available under aCC-BY 4.0 International license.

69. Delaneau O, Zagury J-F, Marchini J. Improved whole-chromosome phasing for disease and population genetic studies. Nat Methods. 2013;10: 5–6. doi:10.1038/nmeth.2307

70. Delaneau O, Marchini J, Zagury JF. A linear complexity phasing method for thousands of genomes. Nat Methods. 2012;9: 179–181. doi:10.1038/nmeth.1785

71. Guindon S, Dufayard J-F, Lefort V, Anisimova M, Hordijk W, Gascuel O. New algorithms and methods to estimate maximum-likelihood phylogenies: assessing the performance of PhyML 3.0. Syst Biol. 2010;59: 307–21. doi:10.1093/sysbio/syq010

72. Bouckaert RR. DensiTree: making sense of sets of phylogenetic trees. Bioinformatics. 2010;26: 1372–3. doi:10.1093/bioinformatics/btq110

73. Bouckaert R, Heled J, Kühnert D, Vaughan T, Wu C-H, Xie D, et al. BEAST 2: A Software Platform for Bayesian Evolutionary Analysis. Prlic A, editor. PLoS Comput Biol. Public Library of Science; 2014;10: e1003537. doi:10.1371/journal.pcbi.1003537

74. Keightley PD, Pinharanda A, Ness RW, Simpson F, Dasmahapatra KK, Mallet J, et al. Estimation of the Spontaneous Mutation Rate in Heliconius melpomene. Mol Biol Evol. 2015;32: 239–243. doi:10.1093/molbev/msu302

75. Owen DF, Chanter DO. Population biology of tropical African butterflies. Sex ratio and genetic variation in Acraea encedon. J Zool. 1969;157: 345–374. doi:10.1111/j.1469-7998.1969.tb01707.x

76. Rambaut A, Drummond AJ, Xie D, Baele G, Suchard MA. Posterior Summarization in Bayesian Phylogenetics Using Tracer 1.7. Susko E, editor. Syst Biol. 2018;67: 901–904. doi:10.1093/sysbio/syy032

Acknowledgements

We are grateful to Godfrey Amoni Etelej, Laura Hebberecht-Lopez and Glennis Julian for support with butterfly rearing. We thank Jenny York, Frank Jiggins and Deborah Charlesworth helpful comments. This work was funded by European Research Council (ERC) European Union Horizon 2020 research and innovation programme grant 646625 (CB), ERC grant 339873 (CDJ, SHM), National Geographic Society Research Grant WW-138R-17 (IJG), and a Royal Society University Research Fellowship (SHM).